

DYNAMIC APERTURE STUDIES FOR THE EIC ELECTRON STORAGE RING*

Y. Nosochkov[†], Y. Cai, Stanford Linear Accelerator Center, Menlo Park, CA 94025, USA
 J. S. Berg, J. Kewisch, Y. Li, D. Marx, C. Montag, S. Peggs, S. Tepikian, H. Witte,
 Brookhaven National Laboratory, Upton, NY 11973, USA
 G. H. Hoffstaetter, J. Unger, Cornell University, Ithaca, NY 14850, USA

Abstract

The electron-ion collider will be constructed at Brookhaven National Laboratory with the goal of providing high luminosity, high average beam polarization, and a wide range of colliding beam energies. One critical requirement is a large dynamic aperture (DA) of the collider rings, in both transverse and momentum dimensions. The ring lattices have been continually optimized to improve the geometric and optics conditions. This paper presents results of the DA studies for the recent lattices of the Electron Storage Ring at different energies, including non-linear chromaticity correction, effects of errors, magnet field quality, and orbit correction options.

INTRODUCTION

The electron ion collider (EIC) [1, 2] will be built at Brookhaven National Laboratory. The important design goals are the high luminosity up to 10^{34} cm⁻²s⁻¹, the high average beam polarization, and a wide range of colliding beam energies. There are separate electron and hadron storage rings with up to two interaction points (IP6 and IP8). A small beam transverse size at IP is achieved using low-beta optics in these interaction regions (IR). Attaining a sufficient beam lifetime requires that dynamic aperture (DA) in both transverse and momentum dimensions reaches the size of 10σ of beam distribution. This is a challenge because the IR final focus quadrupoles, where beta functions are very high, generate huge linear and non-linear chromaticity and cause strong error effects, which reduce the DA. Proximity of the design betatron tunes to integer values further enhances the impact of these effects.

In this paper, we present the studies for the electron storage ring (ESR). Several lattice configurations have been designed corresponding to electron energies of 18 GeV, 10 GeV and 6 GeV with one or two IPs. The 18 GeV lattice is the most challenging due to:

1. The strong 90° FODO arc optics, which is required in order to counterbalance the emittance growth with energy.
2. The large rms energy spread of $\sigma_p \approx 0.1\%$. The 10 GeV and 6 GeV configurations use the weaker 60° arc optics, where the rms energy spread is about 0.06%.

The two-IP lattices have more high-beta IR quadrupoles, thus creating the strongest chromatic and magnet error effects. To achieve the specified $10\sigma_p$ range, a sophisticated

non-linear chromaticity correction scheme [3] has been developed. The DA with magnet errors is evaluated in tracking simulations without beam-beam effects. For cost-efficient realization of the ESR, there is an interest in reusing available magnets from other projects. The impact of these magnets field quality on the DA is verified, and the related correction scheme options are discussed.

CHROMATICITY

The chromaticity correction scheme for the most challenging 18 GeV lattice with two IPs is described in detail in [3, 4]. It consists of multi-family chromatic sextupoles, located in the arcs, and harmonic sextupoles in straight sections. The scheme provides efficient correction of the non-linear chromaticity, including the large first and second order W-functions generated in the low-beta IRs, the second order dispersion, and the third order geometric resonance driving terms, reaching the desired momentum acceptance of $\delta = \Delta p/p = \pm 1\%$.

To minimize the impact of sextupole non-linear fields on the on-momentum DA, the sextupoles in the 18 GeV 90° arcs are arranged in -I pairs, hence their non-linear geometric aberrations are cancelled [5]. Similarly, the -I pairs are used in the 60° arcs of the lower energy lattices; however, their arrangement is different. As a result, different sextupole families must be used in the 90° and 60° lattices, even though both corrections are based on the same principles. Since both configurations must use the same physical magnets, the sextupole power supplies must be compatible with the different schemes.

Here, we describe details of the chromaticity correction in the 10 GeV lattice with the 60° arcs and one or two low-beta IRs. A similar strategy applies to the 6 GeV lattice. Beta functions in the 10 GeV lattice with two low-beta IRs are shown in Fig. 1. Note that the IR optics is not symmetric relative to the IP. The six periodic arcs and six straight sections (all called IRs) are labelled according to the clock. For these studies, the betatron tune is $\nu_x = 43.12$, $\nu_y = 38.1$, and the beta functions at the IP6, IP8 are $\beta_x^* = 45$ cm, $\beta_y^* = 5.6$ cm [6].

The IR high-beta final focus quadrupoles create significant non-linear chromaticity in the form of chromatic beta beating and high order tune shift, which severely limit the momentum range. Due to the complexity of the IR design, which must meet both geometric and optical requirements, including crab cavities, spin rotator sections, and spectrometer dipoles, it does not have space for a conventional local chromaticity correction scheme based on non-inter-

* Work supported by Brookhaven Science Associates, LLC under Contract No. DE-SC0012704, and by the U.S. Department of Energy under Contract No. DE-AC02-76SF00515.

[†] yuri@slac.stanford.edu

leaved -I sextupole pairs [7]. Therefore, the IR chromaticity correction has to be carried out by sextupoles in the arcs, called a semi-local correction.

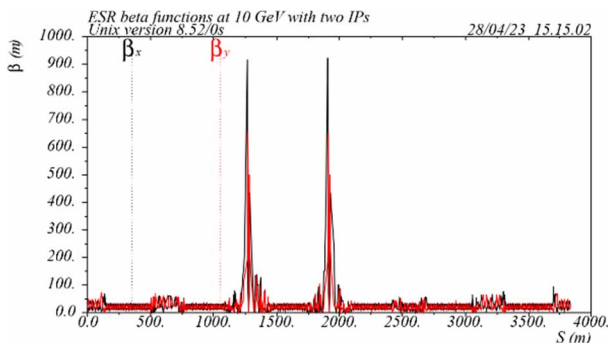


Figure 1: ESR beta functions at 10 GeV with two IRs.

Schematic of the semi-local sextupole scheme on one side of the IP is shown in Fig. 2. Here, the six independent sextupole families, constructed of -I pairs, are placed periodically in the adjacent to the IR 60° arc. An independent set of six sextupole families is used on the other side of the IR. The main function of these sextupoles is to cancel the large chromatic beta beating originating from the IR high-beta quadrupoles by creating an opposite chromatic beta wave in the same phase. This is achieved by optimizing the sextupole strengths and the IR phase advance, indicated in Fig. 2 by “phase trombone”. The chromatic beta beating is traditionally described by the Montague functions [8] or by the W-functions. The linear chromaticity in this region is also optimized for the best non-linear correction.

In this scheme, ideally, the IP W-functions are matched to zero, and the large W-functions created by the IR high-beta quadrupoles are gradually cancelled in the adjacent arcs. However, the complete ring correction, which includes chromaticity from other regions, may work better when these conditions are met approximately. The correction optimization is performed with the LEGO code [9], which is able to compute the lattice function derivatives with momentum to an arbitrary order [10].

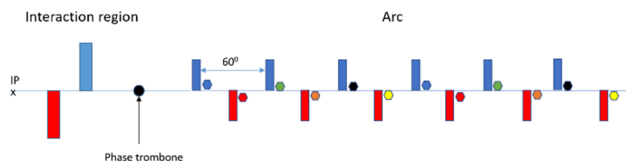


Figure 2: Schematic of the 10 GeV semi-local sextupole scheme on one side of IP, where the columns are quadrupoles and the hexagons are six-family sextupoles.

The optimal correction of the 10 GeV lattice with a single IR6 required an extension of the semi-local scheme to two arcs per each side of the IR6. The resulting cancellation of the IR large W-functions in these four arcs is shown in Fig. 3. The remaining two arcs contain two-family sextupoles for correction of linear chromaticity, which is maintained at +1 in both planes for the whole ring. Optimization of the strengths of the 14 sextupole families along with the phase advance in the IR6 and other straight sections yields the desired $10\sigma_p$ momentum range of 0.6%.

Application of the semi-local scheme to the two-IP lattice with low-beta IR6 and IR8 is more challenging since there is only one arc-7 between the IRs. Therefore, sextupoles in this arc must compensate both IRs. In this case, the semi-local scheme uses 18 sextupole families in arcs 5, 7, and 9. LEGO optimization determined that another six chromatic sextupole families are necessary in the remaining three arcs for both linear and non-linear correction. One more sextupole is included in arc-11 to minimize the second order dispersion. In total, 25 sextupole families are used in the 10 GeV lattice with two IPs. The phase advance in the IRs and other straight sections is also optimized for the maximum momentum range of 0.7%. Figure 4 shows the resulting dependence of the betatron tune and DA of this lattice without errors vs δ . Note that due to the use of -I sextupole pairs, the on-momentum DA is reasonably large even without harmonic sextupoles. The radiation damping effects are included; and the rms beam size (σ) is determined conservatively for a fully coupled emittance of $\epsilon_x = 22$ nm and $\epsilon_y = \epsilon_x / 2$.

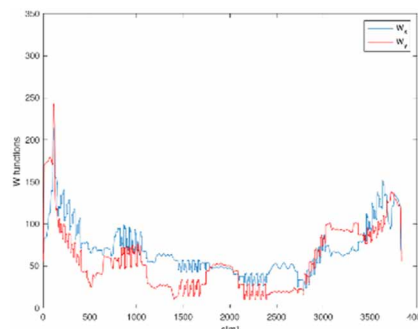


Figure 3: W-functions in the 10 GeV lattice with the low-beta IR6, starting from IP6.

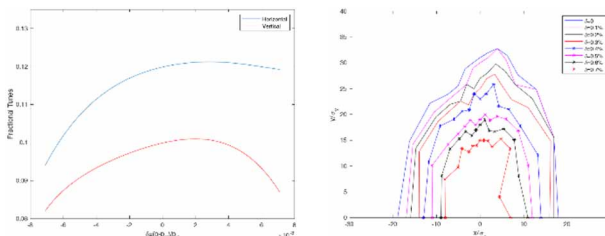


Figure 4: Tune vs δ , and DA without errors at $\delta = 0$ to 0.7% in the 10 GeV lattice with the low-beta IR6 and IR8.

DYNAMIC APERTURE WITH ERRORS

In this section, we discuss the on-momentum DA with magnet errors for the ESR lattices (version 5.6), including options of using available magnets from other projects.

The DA is calculated in particle tracking simulations with LEGO. Misalignment, strength errors, and magnet non-linear field (multipoles) are applied to dipoles, quadrupoles and sextupoles, including BPM misalignment. The errors make distortions of beam orbit, dispersion, beta functions, x - y coupling, chromaticity, betatron tune, and excite non-linear resonances. The strongest effects come from errors in the high-beta magnets near the IP.

To avoid unstable optics and minimize the DA reduction, the error effects are corrected using the correction schemes

in LEGO. The betatron tune and linear chromaticity are maintained at their design values using two-family arc quadrupoles and sextupoles. The orbit is minimized with dipole correctors and BPMs, where the vertical correctors are also used to minimize the vertical dispersion. The transverse coupling is corrected using the technique of sextupole vertical offsets, which create the skew quadrupole effects. Finally, beta function distortions are minimized with adjustment of quadrupole strengths. The SVD method is used for finding the most efficient set of correctors. To avoid unstable optics conditions, the errors are added in small steps, while applying the corrections at each step, until the full error values are reached.

After the correction, a 2000-turn tracking is performed for 10 seeds of random errors. Synchrotron oscillations and effects of non-linear fringe field in quadrupoles and dipoles [11] are included. The DA size is defined as the minimum DA among the 10 seeds. Simulations without radiation effects yield a pessimistic DA estimate, while the radiation damping reduces the electron amplitude, thus decreasing the impact of non-linear field resulting in larger DA.

We use conservative misalignment and strength errors based on the PEP-II [12] values. Magnet rms x, y offsets and roll angles are 0.2 mm and 0.5 mrad, respectively. Smaller rms x, y errors of 0.1 mm are needed for the sensitive high-beta IR quadrupoles; this value is also used for BPMs. The rms strength error is 0.1% in dipoles and quadrupoles, 0.2% in sextupoles, and 0.05% in the high-beta quadrupoles and dipoles near IP. Typical residual rms distortions after correction are: 0.3-0.4 mm of orbit, ~ 1 m of $\Delta\beta$, ~ 10 cm of horizontal and ~ 3 cm vertical dispersion.

Various options for the magnet non-linear field have been examined. Measured multipoles of PEP-II [12], HERA [13], and APS [14-16] magnets have been used for the studies as well as the multipoles based on the ESR magnet design [17]. There is a number of HERA and APS magnets, which may be available for a possible reuse in the ESR. The measured multipoles in the APS quadrupoles and sextupoles are shown in Fig. 5.

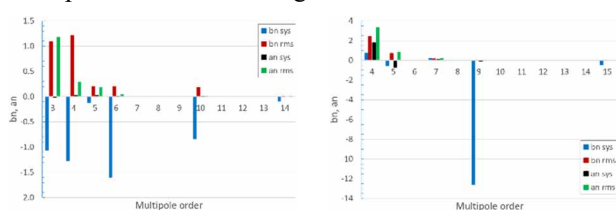


Figure 5: Systematic and random (rms) multipoles in the APS quadrupoles (left) and sextupoles (right) at $r = 25$ mm.

In the study, the multipoles in the above options are applied to all magnets except the high-beta IR magnets. Multipole tolerances in the high-beta quadrupoles and dipoles near IP are determined separately due to their strong impact on the DA.

Dynamic aperture with errors for one-IR lattices at 10 GeV and 18 GeV are shown in Fig. 6. The multipole field in these cases is based on the measured HERA quadrupoles, the new ESR dipoles, and the measured PEP-II sextupoles. The simulations are without radiation effects,

thus yielding the pessimistic DA estimate. The DA is 11.9σ at 10 GeV and 10.1σ at 18 GeV, where the beam size is determined for the ideal emittance of $\epsilon_x = 22$ nm-rad at 10 GeV and 28 nm-rad at 18 GeV, and $\epsilon_y = \epsilon_x / 2$.

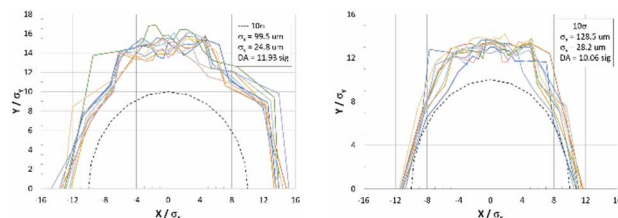


Figure 6: DA at IP6 for 10 seeds of errors without radiation for one-IR lattices at 10 GeV (left) and 18 GeV (right), where multipoles from the HERA quadrupoles are used.

Dynamic aperture for the more challenging two-IR lattice at 18 GeV is shown in Fig. 7 for the multipole options based on 1) HERA quadrupoles and ESR sextupoles, and 2) APS quadrupoles and sextupoles, where multipoles in dipoles are from the ESR magnet design. The LEGO corrections were optimized for maximum DA. The HERA and APS multipole models yield similar DA of $\sim 10\sigma$, estimated without radiation for the ideal fully coupled emittance of $\epsilon_x = 28$ nm-rad.

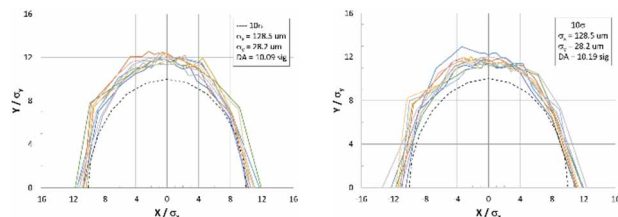


Figure 7: DA at IP6 for 10 seeds of errors without radiation for two-IR lattice at 18 GeV for the options of HERA quadrupoles (left), and APS quadrupoles and sextupoles (right).

Assuming a reuse of the APS dual-plane correctors, which quantity is limited, we examined the scheme where these correctors and dual-plane BPMs are included only at defocusing quadrupoles, except in the ± 100 m area around IP, where they are at all quadrupoles. This was compared to more traditional schemes with a single-plane corrector at each quadrupole, and dual-plane BPMs at either all quadrupoles or only at defocusing quadrupoles. The result of not having correctors and BPMs at focusing quadrupoles is an increase of average rms x -orbit by $\sim 70\%$ and average x -emittance by $\sim 9\%$ compared to the scheme with correctors and BPMs at all quadrupoles. The slight decrease of the DA due to the larger emittance should be considered when deciding on the optimal correction scheme.

This study demonstrates that the required 10σ DA in both transverse and momentum dimensions has been achieved with the described chromaticity correction scheme and a careful correction of errors, including the options of using the available magnets from HERA or APS.

REFERENCES

- [1] J. Beebe-Wang *et al.*, "Electron-ion collider: conceptual design report", Brookhaven National Laboratory, Thomas Jefferson National Accelerator Facility, 2021. www.bnl.gov/EC/files/EIC_CDR_Final.pdf
- [2] C. Montag *et al.*, "Design status of the electron-ion collider", presented at IPAC'23, Venice, Italy, May 2023, paper MOPA049, this conference.
- [3] Y. Cai *et al.*, "Optimization of chromatic optics in the electron storage ring of the electron-ion collider", *Phys. Rev. Accel. Beams*, vol. 25, p. 071001, Jul. 2022. doi:10.1103/PhysRevAccelBeams.25.071001
- [4] Y. Nosochkov *et al.*, "Dynamic aperture of the EIC electron storage ring", in *Proc. IPAC'22*, Bangkok, Thailand, Jun. 2022, paper WEPOPT043, pp. 1950-1953. doi:10.18429/JACoW-IPAC2022-WEPOPT043
- [5] K. L. Brown and R. V. Servranckx, "Optics modules for circular accelerator design", SLAC-PUB-3957, May 1986.
- [6] Y. Luo *et al.*, "Optimizing the design tunes of the electron storage ring of the electron-ion collider," presented at IPAC'23, Venice, Italy, May 2023, paper MOPA047, this conference.
- [7] M. Donald *et al.*, "Localized chromaticity correction of low-beta insertions in storage rings", in *Proc. PAC'93*, Washington, D.C., USA, May 1993, pp. 131-133.
- [8] B. W. Montague, "Linear optics for improved chromaticity correction", CERN-LEP-NOTE-165, Jul. 1979.
- [9] Y. Cai, M. Donald, J. Irwin, and Y. Yan, "LEGO: a modular accelerator design code", in *Proc. PAC'97*, Vancouver, B.C., Canada, May 1997, pp. 2583-2585.
- [10] Y. Cai, "Symplectic maps and chromatic optics in particle accelerators", *Nucl. Instrum. Methods*, vol. 797, pp. 172-18, 2015.
- [11] Y. Cai and Y. Nosochkov, "Dynamical effects due to fringe field of the magnet in circular accelerators", in *Proc. PAC'05*, Knoxville, TN, USA, May 2005, paper MPPE025, pp. 1907-1909.
- [12] "PEP-II: an asymmetric B factory. Conceptual design report", SLAC-418 Office of Scientific and Technical Information (OSTI), Jun. 1993. doi:10.2172/10112145
- [13] "HERA - A proposal for a large electron-proton colliding beam facility at DESY", DESY-HERA-81-10, 1981. doi:10.3204/PUBDB-2017-01301
- [14] S. H. Kim, K. Kim, C. Doose, R. Hogrefe, and R. Merl, "Magnetic measurements of the storage ring quadrupole magnets for the 7-GeV Advanced Photon Source", in *Proc. PAC'93*, Washington, D.C., USA, May 1993, pp. 2805-2807.
- [15] S. H. Kim, D. W. Carnegie, C. Doose, R. Hogrefe, K. Kim, and R. Merl, "Statistical analyses of the magnet data for the Advanced Photon Source storage ring magnets", in *Proc. PAC'95*, Dallas, Texas, USA, May 1995, pp. 1310-1315.
- [16] C. L. Doose, private communication, Mar. 2023.
- [17] H. Witter, private communication, Jun. 2020.